REPORT DOCUMENTATION PAGE

Form Approved
OMB No. 0704-0188

1. REPORT DATE *(MM/DD/YYYY)*	**2. REPORT TYPE**	**3. DATES COVERED** *(From - To)*
	Manuscript	

4. TITLE AND SUBTITLE
Reduced Micro-cracking in PMR-15 Type Resin Modified with Silsesquioxane Diamine Monomer

5a. CONTRACT NUMBER
In-House

5b. GRANT NUMBER

5c. PROGRAM ELEMENT NUMBER

6. AUTHOR(S)
Jason T. Lamb, Gregory R. Yandek, Timothy S. Haddad, Michael D Ford, Andrew J. Guenthner, Joseph M. Mabry

5d. PROJECT NUMBER

5e. TASK NUMBER

5f. WORK UNIT NUMBER
Q16J

7. PERFORMING ORGANIZATION NAME(S) AND ADDRESS(ES)

Air Force Research Laboratory
Propellants Branch
10 E Saturn Blvd
Edwards AFB, CA 93524

8. PERFORMING ORGANIZATION REPORT NO.

9. SPONSORING / MONITORING AGENCY NAME(S) AND ADDRESS(ES)

Air Force Research Laboratory
Rocket Propulsion Division
5 Pollux Drive
Edwards AFB, CA 93524

10. SPONSOR/MONITOR'S ACRONYM(S)
RQRS

11. SPONSOR/MONITOR'S REPORT NUMBER(S)
AFRL-RQ-ED-JA-2017-033

12. DISTRIBUTION / AVAILABILITY STATEMENT
DISTRIBUTION STATEMENT A. Approved for public release. Distribution is unlimited.

13. SUPPLEMENTARY NOTES
Public Affairs Clearance Number: 17127; Clearance Date: 16 Mar 2017.
This material is based on work supported by the Air Force Research Laboratory.

14. ABSTRACT
With the goal of replacing methylene dianiline (MDA) in PMR-15 (polymerizable monomeric reactant), a known toxin to humans, a thermally stable polyhedral oligomeric silsequioxane (POSS) dianiline featuring an aromatic periphery was co-polymerized as a "dropin" replacement. The chain length of the experimental oligomers was varied to study effects of cross-link density and nadic endcap concentration. It was shown that the bulky monomer addition improved moisture resistance (80% decrease in ultimate moisture absorption) and processability (uncured glass transition temperature (Tg) and rheology) were improved. Uncured Tg values decreased by as much as 85 °C and complex viscosity decreased by three orders of magnitude. However, thermal properties such as cured Tg and long-term thermal oxidative stability (TOS) along with composite strengths were hindered. Shortening of the chain length, which increases cross-link density, is shown to improve cured Tg. The decreased chain length causes increased nadic endcap concentration and lowers the thermal stability of the polyimide.

15. SUBJECT TERMS
PMR-15 replacement, methylene dianiline, high temperature polymer matrix composites, polyhedral oligomeric silsesquioxane, POSS, polyimide, micro-cracking

16. SECURITY CLASSIFICATION OF:			**17. LIMITATION OF ABSTRACT**	**18. NUMBER OF PAGES**	**19a. NAME OF RESPONSIBLE PERSON**
					Kamran Ghiassi
a. REPORT	**b. ABSTRACT**	**c. THIS PAGE**			**19b. TELEPHONE NO** *(include area code)*
Unclassified	**Unclassified**	**Unclassified**	SAR	37	

Standard Form 298 (Rev. 8-98)
Prescribed by ANSI Std. 239.18

Reduced Micro-cracking in PMR-15 Type Resin Modified with Silsesquioxane Diamine Monomer

Jason T. Lamb[1], Gregory R. Yandek[2*], Timothy S. Haddad[1], Michael D. Ford[1], Andrew J. Guenthner[2], Joseph M. Mabry[2]*

[1]ERC, Inc., Edwards AFB, California 93524, United States

[2]Air Force Research Laboratory, Aerospace Systems Directorate, Edwards AFB, California 93524, United States

Keywords: PMR-15 replacement, methylene dianiline, high temperature polymer matrix composites, polyhedral oligomeric silsesquioxane, POSS, polyimide, micro-cracking

ABSTRACT

With the goal of replacing methylene dianiline (MDA) in PMR-15 (polymerizable monomeric reactant), a known toxin to humans, a thermally stable polyhedral oligomeric silsequioxane (POSS) dianiline featuring an aromatic periphery was co-polymerized as a "drop-in" replacement. The chain length of the experimental oligomers was varied to study effects of cross-link density and nadic endcap concentration. It was shown that the bulky monomer addition improved moisture resistance (80% decrease in ultimate moisture absorption) and processability (uncured glass transition temperature (T_g) and rheology) were improved. Uncured T_g values

decreased by as much as 85 °C and complex viscosity decreased by three orders of magnitude. However, thermal properties such as cured T_g and long-term thermal oxidative stability (TOS) along with composite strengths were hindered. Shortening of the chain length, which increases cross-link density, is shown to improve cured T_g. The decreased chain length causes increased nadic endcap concentration and lowers the thermal stability of the polyimide.

INTRODUCTION

PMR-15, developed by NASA Lewis Research Center in the 1970s, is the aerospace industry's most prolifically utilized high temperature organic matrix composite (OMC) resin for lightweight hot structures in aircraft and other applications [1-4]. PMR-15 chemistry involves the polymerization of the following monomers: methylene dianiline (MDA), 5-norbornene-2,3´-dicarboxylic half acid ester (NE), and 3,3´,4,4´-benzophenonetetracarboxylic diester (BTDE), as shown in Figure 1. The MDA monomer, possessing a single methylene bridge between two aniline groups, is uniquely effective due to its balance between thermal stability (low aliphatic character) and slight flexibility, thus imparting a certain degree of processability to oligomers. The popularity of PMR-15 is based on its unique combination of properties, including manageable processability, high service temperature (max. 288 °C), excellent long-term thermal oxidative stability (TOS), and good mechanical properties including fracture toughness and resistance to micro-cracking.

However, since the early 1980s, it has been recognized that MDA, a key monomer in PMR-15, poses health risks [5-11]. While material solutions are available for lower service temperatures (BMIs), materials for service temperatures similar to those of PMR-15 are notably deficient.

Of the over 50 known reported diamines studied as alternatives to MDA, including those possessing phenyl linkage groups such as ketone, sulfur, sulfone, ether, unsaturated aliphatic

groups, as well as three and four-phenyl ring diamines, none have afforded the combination of high glass transition temperature (T_g), low weight loss after more than 1000 hours at 288 °C, and desirable mechanical properties that the use of MDA provides [12]. Monomers imparting higher T_gs than MDA such as NASA's developed asymmetric class of monomers, most notably 2,2´-dimethylbenzidine (DMBZ), also recently commercialized in PMR chemistry, suffer from lower long-term TOS due to their methyl groups.

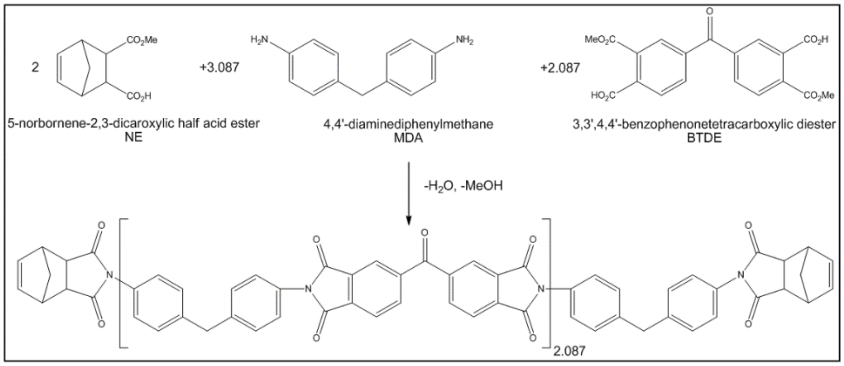

Figure 1. Chemistry of heritage PMR-15.

In order to fill the persistent need for an acceptable MDA replacement, we pioneered a new approach involving a silsesquioxane-based dianiline monomer featuring a silicon-oxygen core and aromatic, thermally stable organic periphery [13]. The core compound that is used to synthesize this dianiline, a polyhedral oligomeric silsesquioxane (POSS) tetrasilanol, is commercially available (Hybrid Plastics, Hattiesburg, MS). Although the toxicity of the subject diamine has not been specifically studied, it is not expected to present toxicity issues due to its relatively high molecular weight and chemical architecture. Several published works have investigated the toxicity of POSS compounds in biological systems [14-19]. In particular, Rotello *et al*. demonstrated that amine-functionalized POSS molecules exhibit very low toxicity to Cos-1 cells derived from monkey kidney tissue, as evidenced by cell vitality after POSS incubation [14]. POSS-containing copolymers have also been investigated for their biocompatibility and

functionality for cardiovascular device applications [16-17, 19], other biomedical devices [18], and recently as a molecular scaffold to engineer tissue replacements for human noses [20].

In previous work, the POSS dianiline monomer was copolymerized with 4,4′-(hexafluoro-isopropylidiene)diphthalic anhydride (6-FDA), 4,4′-oxydianiline (ODA), and phenylethynyl phthalic anhydride (PEPA) endcap, monomers common to PMR chemistries, to produce short chain cross-linkable oligoimides of n_{ave}=4 [21]. The POSS content was systematically altered to yield oligomers possessing no POSS (control) to 3 POSS units on average. Consequently, ODA content also varied. Target molecular weights were achieved and the POSS cage remained intact during oligomer synthesis. The oligomers were cured using standard heat and pressure protocol prescribed for phenylethynyl crosslinking to yield neat resin specimens. Characterization of this suite of polyimides revealed very promising properties including very low melt viscosity, exceptionally low moisture uptake, and only a modest reduction in glass transition temperature.

Using these results as a foundation, this work further investigated the subject POSS dianiline for its viability as a constituent in a polyimide chemically analogous to PMR-15 by synthesizing a nadic end-capped oligomer and characterizing its properties both in the uncured and cured states, as well as in composite form. The results demonstrate that POSS, when copolymerized into the backbone of a thermosetting oligoimide, delivers a property set equivalent or superior to PMR-15, in terms of processability, mechanical properties, and thermal properties including long-term TOS, with the expectation that the monomer will provide a non-toxic multi-functional alternative to MDA for thermosetting polyimides.

MATERIALS AND METHODS

Materials. Methanol (MeOH) and tetrahydrofuran (THF) were obtained from Fischer Scientific and were used as received. 3,3,’,4,4’-benzophenonetetracarboxylic dianhydride and 5-

norbornene-2,3,-dicarboxylic anhydride were obtained from Sigma-Aldrich and used as received while stored in a dry, N_2-environment glove box. 4,4' methylene dianiline was also obtained from Sigma-Aldrich and was also used as received. IM7 4 harness satin weave carbon fiber fabric was used as received from Hexcel. Polyhedral oligomeric silsesquioxane (POSS) dianiline was synthesized as previously reported [21].

Oligomer Synthesis. Nadic endcaps were utilized in all routes to preserve the resin curing temperature characteristics of PMR-15. The basic approach is illustrated in Figure 2. In the primary strategy, the POSS dianiline simply replaced MDA in the heritage PMR-15 chemistry. Because the POSS monomer is larger than MDA, it was expected to increase the molecular weight between crosslinks which was in turn expected to reduce T_g in similar fashion to what had been previously observed. To mitigate this reduction in T_g, we investigated varying oligomer length (*n*) between 0 and 2, as shown in Figure 2, to effectively increase the crosslink density of cured oligomers. The 2N oligomer is derived from nearly equivalent stoichiometry to that used in PMR-15. Blends of the oligomers were also investigated, in an effort to tune the crosslink density and T_g.

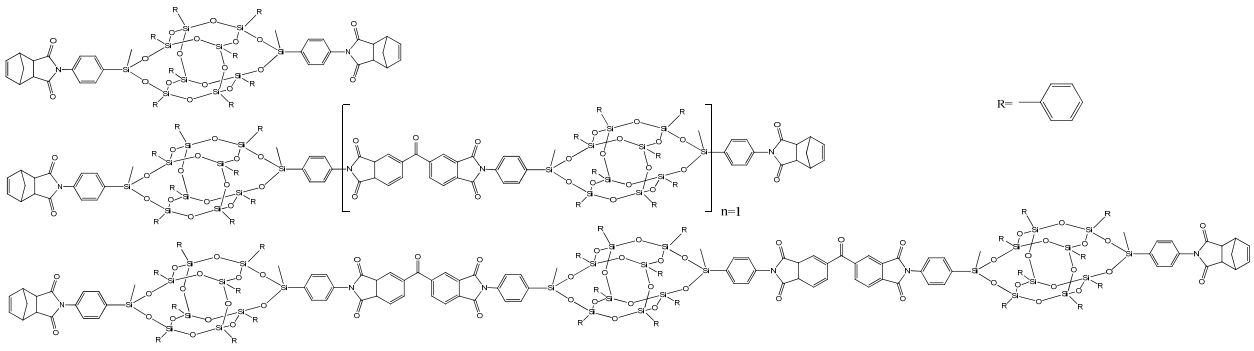

Figure 2. Reaction Scheme 1: target PMR oligomers featuring NE, BTDE, and POSS substituted for MDA with varying repeat units n (BTDA-POSS); 0N (top), 1N (middle), and 2N (bottom).

The nomenclature for the group of oligomers investigated in this program and used in the remainder of this paper is shown in Table 1. A repeat *n* is represented by BTDA or BTDE and a dianiline.

Table 1. Oligomer nomenclature utilized for the purposes of this paper. The constituent monomers are BTDA (benzophenonetetracarboxylic dianhydride), BTDE (benzophenonetetracarboxylic diester), MDA (methylene dianiline), POSS (polyhedral oligomeric silsesquioxane).

$BTDE_{2.087}MDA_{3.087}NA_{2.087}$	PMR-15 (MeOH)
$BTDA_{2.087}MDA_{3.087}NA_{2}$	PMR-15 (THF)
$POSS_{1}NA_{2}$	0N
$BTDA_{1}POSS_{2}NA_{2}$	1N
$BTDA_{2}POSS_{3}NA_{2}$	2N

PMR-15 Synthesis in Methanol~5g Scale: In a dry nitrogen purged glove box, 2.016 g BTDA and 0.985 g 5-norbornene-2,3-dicarboxylic anhydride (NA) were weighed in a 50 mL round bottom flask. The flask was removed from the glove box and 17 mL MeOH was added. The mixture was refluxed at 70 °C for 2 hours, during which the powders were solubilized into a yellow liquid. The solution was removed from the heat and allowed to cool to room temperature. Once at room temperature, 1.836 g MDA was added while stirring. The MDA dissolved in approximately five minutes and the solution (darker shade of yellow) was left to stir for 1 hour. The solvent was then evaporated using rotary evaporation and 5.218 g yellow amic acid powder was recovered. To imidize, the powder was then added to a petri dish and placed into a 200 °C oven for 2 hours, then 230 °C for 30 minutes to yield an orange powder.

PMR-15 Synthesis in THF~5g Scale: In a dry nitrogen purged glove box, 1.8363 g MDA was dissolved in 10 mL THF, 2.0159g BTDA was dissolved in 70 mL THF, and 0.9851 g NA was dissolved into 10 mL THF, in separate round-bottom flasks. The BTDA solution was poured slowly (but not dropwise) into the MDA solution while stirring. When added, the solution became orange in color and when all of the solution was added a pale yellow precipitate appeared. Then, the NA solution was added in the same manner with no apparent change in color or solubility. This was left to stir overnight. The next day, the solution was a clear yellow liquid. The solvent was evaporated using rotary evaporation and 4.1090 g yellow amic acid powder was recovered. To imidize, the powder was then added to a petri dish and placed into a 200 °C oven for 2 hours, then 230 °C for 30 minutes to yield an orange powder.

2N Synthesis in THF~3g scale: In a dry nitrogen purged glove box, three solutions were made: 2.468g *meta*/*para* POSS dianiline with 25 mL THF, 0.202 g NA with 2 mL THF, and 0.397 g BTDA with 4 mL THF. While stirring, the BTDA solution was added to the POSS dianiline solution. The resulting solution became yellow and darkened as more solution was added. After 1 hour of stirring, the NA solution was added and no change in appearance occurred. This was left to stir overnight. The yellow solution was then evaporated using rotary evaporation and 2.423 g yellow amic acid powder was recovered. To imidize, the powder was then added to a petri dish and placed into a 200 °C oven for 2 hours, then 230 °C for 30 minutes to yield an orange powder.

1N Synthesis in THF~3g Scale: In a dry nitrogen purged glove box, three solutions were made: 2.468 g *meta*/*para* POSS dianiline with 25 mL THF, 0.303 g NA with 2 mL THF, and 0.298 g BTDA with 4 mL THF. While stirring, the BTDA solution was added to the POSS dianiline solution. The resulting solution became yellow and darkened as more solution was added. After 1 hour of stirring, the NA solution was added and no change in appearance occurred. This was

left to stir overnight. The yellow solution was then evaporated using rotary evaporation and 2.423 g yellow amic acid powder was recovered. To imidize, the powder was then added to a petri dish and placed into a 200 °C oven for 2 hours, then 230 °C for 30 minutes to yield an orange powder.

POSS di-Nadic Synthesis (0N) in THF~3g Scale: In a dry nitrogen purged glove box, two solutions were made: 2.461 g POSS dianiline with 25 mL THF and 0.605 g NA with 6 mL THF. While stirring, the NA solution was added to the POSS solution with no change in color (clear). The solution was left to stir overnight. The solution was then evaporated using rotary evaporation and 2.490 g white amic acid powder was recovered. To imidize, the powder was then added to a petri dish and placed into a 200 °C oven for 2 hours, then 230 °C for 30 minutes to yield an orange powder.

Characterization Methods

Nuclear Magnetic Resonance spectroscopy (NMR). All ^{1}H and ^{13}C NMR spectra were obtained from a Bruker 300 MHz FT-NMR. DMSO-d_6 was used as the solvent. Chemical shifts are reported in tables 2 and 3. The spectra was referenced to DMSO-d_6

Differential Scanning Calorimetry (DSC). DSC experiments were carried out on a TA Instruments Q200 DSC. Hermetically sealed aluminum T-Zero DSC pans were loaded with 10-20 mg of imide powder. The experiments were performed under a nitrogen environment at a purge rate of 50 mL/min. An initial ramp of 10 °C/min to 250 °C from RT was implemented to eliminate any residual solvent or water and to allow the powder to flow to form good contact with the bottom of the pan. The samples were then equilibrated at 40 °C and ramped again at 10 °/min to 315 °C. The material was then held at this temperature for 2 hours to promote curing and subsequently equilibrated at 40 °C. The final temperature ramp was executed at 10 °C/min to 400°C.

Thermal Gravimetric Analysis (TGA). TGA experiments were performed on a TA Instruments Q5000 TGA. Experiments were conducted under both air and nitrogen atmospheres. Temperature ramps were implemented between 25 °C and 900 °C (although some experiments only went to 600°C) at a rate of 1 °C/min and 10 °C/min.

Rheology. Rheological experiments were carried out on a TA Instruments Discovery DHR3 rheometer. The samples were loaded onto 25 mm stainless steel parallel plates with a gap of 0.750 mm. During the oscillatory experiments, the strain amplitude was set to 1% and angular frequency was ramped from 0.1 to 100 rad/s. All experiments were carried out at 250 °C.

Thermomechanical Analysis (TMA). TMA experiments were conducted using a TA Instruments Q400 TMA. A quartz expansion-type probe was used and the furnace was purged with a nitrogen atmosphere. Initially, a force of 0.2000 N was implemented and the temperature was equilibrated at 100 °C. Force was modulated at 0.05 Hz at an amplitude of 0.10 N. The temperature was then cycled between 200 °C and 100 °C for two iterations. The temperature was then ramped at 5 °C/min to 360-400 °C, cooled at 5 °C/min to 100 °C, and again ramped at 5 °C/min to 360-400 °C. The cured glass transition temperature was ascertained from the last temperature ramp.

Density. Density measurements were performed using a Mettler-Toledo Density Kit for an MS-S Analytical Balance on 0.5" circular discs (further information on disc preparation is provided in Supporting Information). The liquid used was ethanol. Three measurements were taken and the average is presented.

Moisture Uptake. A 2 L Erlenmeyer flask was filled with approximately 1750 mL of de-ionized water and heated until boiling. Specimen discs were thoroughly dried in a vacuum oven for 3 days or until weight stabilization occurred. All specimens were weighed and then placed into the flask. At approximately 1 hour intervals, the samples were removed from the boiling water, blotted dry

with paper media, blown dry with nitrogen, and weighed. The samples were then placed back into the boiling water and the process was repeated until the eighth interval at which time the samples were left overnight in boiling water before the final weight measurement.

Long-Term Thermal Oxidative Stability (TOS). Long-term isothermal TOS experiments were conducted in a Lindberg Blue M tube furnace, at 316 °C. An air-generator fitted with a flow meter was connected to the tube such that a continuous flow of 100 mL/min of air flowed across the samples. The cured discs were placed onto a graphite boat wrapped in an aluminum mesh to provide support to the discs and to facilitate gas flow above and below the samples. Disk mass measurements were taken at 3-4 day intervals.

Composite Fabrication. One 2"×2"×0.1" and three 1"×5"×0.1" flat laminate composite panels comprised of PMR-15 and 0N in combination with Hexcel IM7, 8 harness satin weave, GP sized carbon fiber woven fabric, were fabricated by curing prepreg consisting of the fabric plies coated with the resin of interest. 60 weight percent solute solutions in methanol for PMR-15. Fabric plies cut to the prescribed dimensions were painted with the solution and dried to render prepreg. In accordance with ASTM D 5687 *Standard Guide for Preparation of Flat Composite Panels with Processing Guidelines for Specimen Fabrication*, resultant plies were stacked in a steel mold to the desired part thickness and cured under pressure by compression molding using the predetermined processing cycle from the preceding characterization efforts, and the commercially recommended cycle for PMR-15. For the POSS-containing panels, bare carbon fabric plies were stacked in a steel mold with dried amic acid powder loaded into the center of the plies. After cure, the parts were removed and systematically characterized.

Composite Characterization. Void content (ASTM D 3171), flexural (ASTM D 7264) and interlaminar shear (ASTM D 2344) mechanical properties were evaluated after sectioning the

panel into test specimens using a diamond wheel composite rotary saw. Mechanical property testing was performed on a 300 kN Tinius Olson load frame. A long-term TOS aging study was also performed, up to 700 hours at 316 °C.

RESULTS AND DISCUSSION

The chemical structures of each of the target oligomers are represented in Figure 3. To compare the target theoretical molecules with the synthesis products, signals corresponding to classes of protons in the ^{1}H NMR spectra for the oligoamic acids prior to imidization were integrated and normalized to the protons in the norbornyl rings in the end caps, and compared with theoretical values. This normalization strategy was chosen because all oligomers should be terminated with norbornyl groups, thus there should be 4 total protons of either aforementioned type for each molecule, and normalization should render an average number average molecular weight (M_n). For PMR-15, the integrations were normalized to the two protons in the methylene of bridge of the norbornyl group (coded purple in Figure 3), while for the POSS-containing materials, normalization was performed through the protons on the ethane groups (coded red in Figure 3). An example of a ^{1}H NMR spectra for the 0N oligoamic acid is shown in Figure 4. The results of normalized integration are presented in Table 2 for PMR-15 and Table 3 for the POSS-containing oligomers. In general, very good agreement was found with the exception of the protons associated with the amic acid group (coded dark blue and orange for the amine and hydroxyl/carboxylic acid groups, respectively, Figure 3), and in some cases the protons attached to phenyl rings. The former finding is likely due to coupling interactions with the carrier solvent, and/or the existence of methoxy groups formed during BTDA esterification, that skew the integrations. Regarding the protons associated with phenyl rings, which are measured to be significantly higher than theoretical (~by 1.5), are located within the spectral range of 6.6-8.3 ppm which is overlapped due

to the number of protons with similar electronic environments, possibly leading to errors with software integration, or the average molecular weight between terminal groups is skewed high due to abnormal polydispersity, or the average molecular weight is indeed higher than that targeted. The protons coded as green are also measured to be higher than theoretical, and since those protons are either associated with the norbornyl groups and the methylene bridge of MDA, any variance should be associated with increased molecular weight due to the presence of higher than expected MDA segments. Despite the possibility of high molecular weight, the cured glass transition of the PMR-15 synthesized in this study is the same as that reported in the literature, which will be discussed later in the resin characterization section, and unlike PMR-15, this series of oligomers was synthesized in THF due to the insolubility of the POSS monomer in methanol.

The POSS-containing oligoimides provide additional insight into the nature of this chemistry. The expected and measured integrations for 0N are in very good agreement, while those of 1N and 2N suggest higher average molecular weight than that which was targeted. It is possible that the use of BTDA, not present in 0N, is complicating to the chemistry. Nonetheless, this NMR analysis provides reasonable confidence that the target molecules were successfully synthesized without significant compositional anomalies, and target average molecular weights were achieved or exceeded.

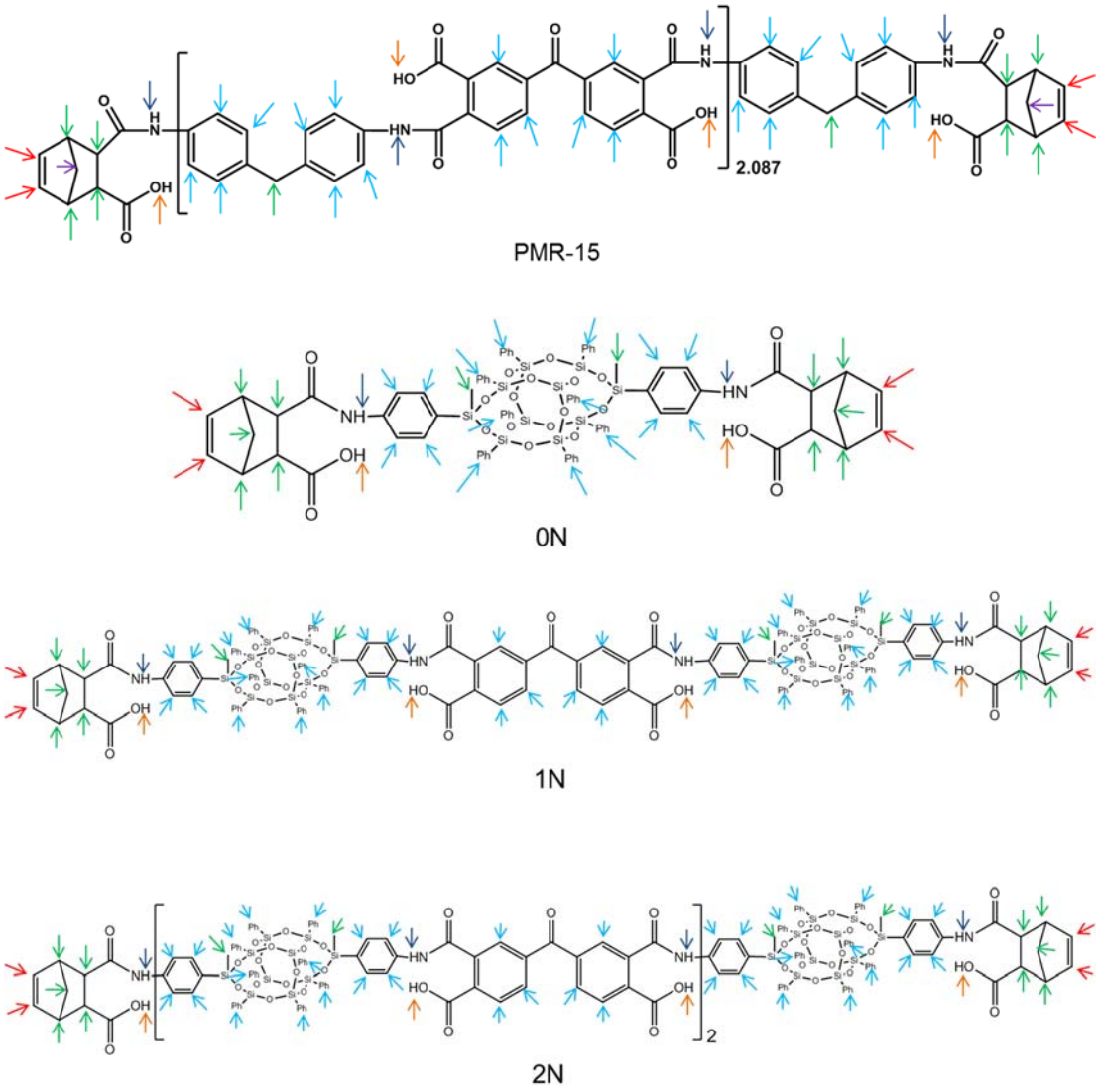

Figure 3. Molecular structures of the amic acids of PMR-15, 0N, 1N, and 2N. Colored arrows correspond to the NMR assignments in Tables 2 and 3.

It is also very informative to examine the ^{29}Si spectra for the POSS-containing materials in relation to the spectra for the POSS dianiline starting material, as it provides diagnostic information pertaining to the integrity of the POSS cage throughout the various stages of material treatment, including the synthesis of the oligoamic acids and the thermal imidization of the amic acid groups. This diagnostic is also aided by the simplicity of the spectra, as shown in Figure 5, where three regions of peaks are prevalent. The T silicon atoms (those with attached phenyl groups and three oxygen bonds) exhibit peaks in the -78 to -80 ppm region, while the D silicon atoms (two oxygen bonds) are identified by the peak at -30 ppm. In terms of chemical and presumably thermal stability, the T-type Si atoms are more stable than the D-type Si atoms, and Si-C bonds are weaker than Si-O. Cage integrity can be compromised by the presence of basic groups, especially at elevated temperature, therefore thermal imidization was identified as a high risk at the inception of the program. During imidization, oligoamic acid is heat treated at 200 °C for 2 hours and 230 °C for 30 minutes, where the amic acid rings closes to form an imide group, liberating water and methanol, both being basic species that can attack the D silicon atoms. However, as can be seen in Figure 5, the NMR spectra reveal that the D silicon atoms' electronic environment remains largely unchanged during oligomer synthesis and thermal imidization, representing a very positive result.

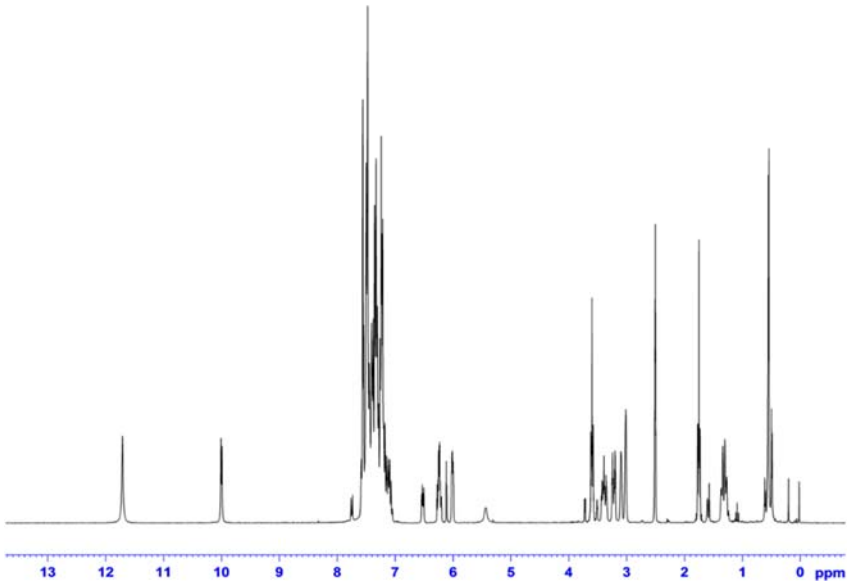

Figure 4. ^{1}H NMR spectra for 0N oligoamic acid. The region between 7-8 ppm features the highest intensity and greatest concentration of peaks due to the number of protons covalently attached to phenyl groups.

Table 2. Expected and measured integrated ^{1}H NMR peak intensities for the PMR-15 oligoamic acid.

Region	PMR-15 (MeOH)		PMR-15 (THF)	
	Expected	Measured	Expected	Measured
6.0 – 6.25ppm	4	4.96	4	4.06
6.6 – 8.3ppm	37.22	58.33	37.22	41.68
1.25ppm	4	4	4	4
2.9 - 3.45ppm; 3.7 - 4.0ppm	14.17	15.92	14.17	14.53
9.8ppm	6.17	1.43	6.17	1.93
10.5ppm	6.17	0.12	6.17	4.40

Table 3. Expected and measured integrated ^{1}H NMR peak intensities for the 0N, 1N, and 2N oligoamic acids.

	0N		1N		2N	
Region	Expected	Measured	Expected	Measured	Expected	Measured
5.9 – 6.3ppm	4	4	4	4	4	4
7.0 – 8.0ppm	48	48.45	102	108.63	156	169.14
0 – 1.6ppm; 3.0-3.5ppm	18	17.92	24	28.80	30	35.65
10ppm	2	1.51	2	0.64	6	0.71
11.75ppm	2	1.97	2	1.82	6	3.76

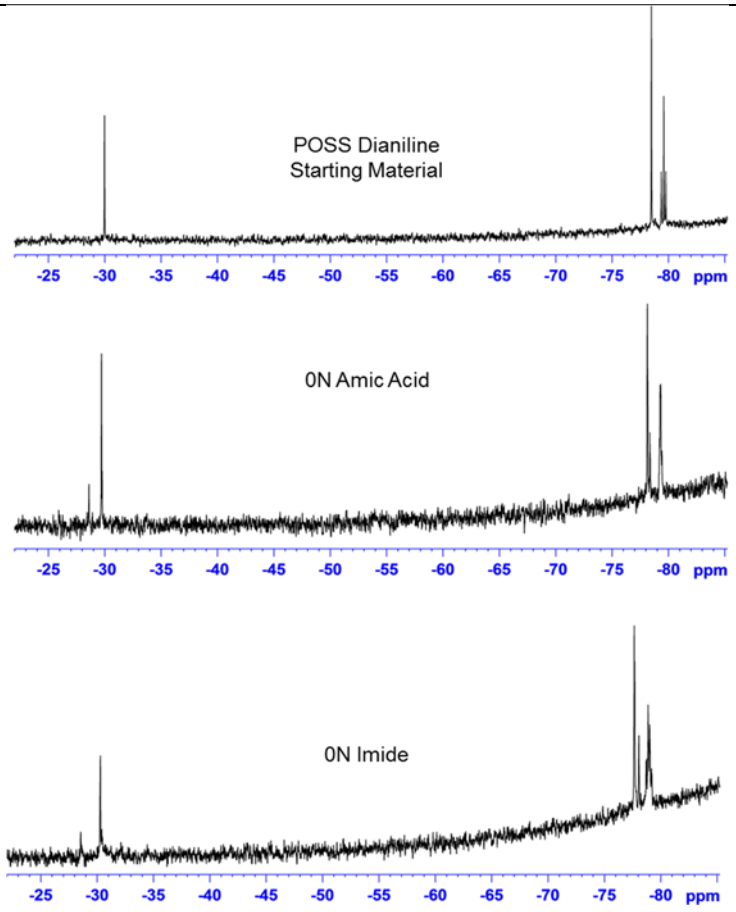

Figure 5. ^{29}Si NMR spectra for the POSS dianiline starting monomer, 0N amic acid, and 0N imide.

Resin Characterization. DSC thermograms corresponding to the uncured oligoimides after an initial ramp to 250 °C to eliminate any residual solvent are shown in Figure 6. In all four materials, inflections are clearly visible indicating a transition from glassy to more fluid-like behavior. The T_g of PMR-15 is 200 °C, equivalent to that reported in the literature [1]. Co-oligomerization with POSS dianiline, replacing MDA, reduces the T_g as a function of POSS content (2N>1N>0N), but this observation also must have dependencies on oligomer molecular weight (2N>1N>0N) and inter-molecular packing.

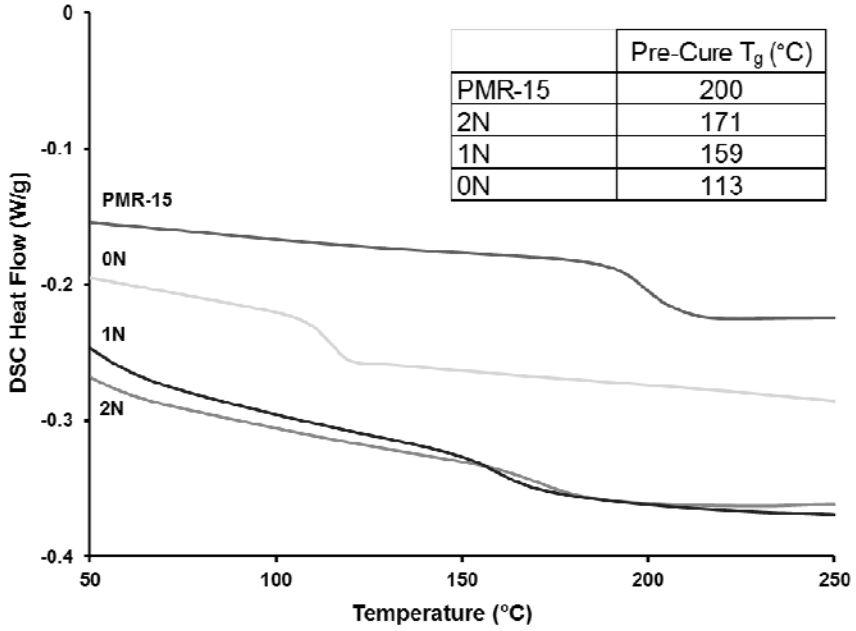

Figure 6. Differential scanning calorimetry (DSC) thermograms of all uncured oligoimides. Quantified pre-cured glass transitions are tabulated in the inset.

The post-cure DSC thermograms of the same specimens after heat treatment at 315 °C for ninety minutes (recommended cycle for PMR-15) are plotted in Figure 7. Again, the T_g of PMR-15 is equivalent to that reported in the literature. Immediately following the transition, the PMR-15 signal becomes exothermic, possibly caused by residual cure occurring after strong segmental

motion is induced, but is more strongly a result of the inception of network degradation first through the products of norbornyl cross-linking [22]. In comparison, the T_gs of the POSS-containing cured thermosets are weak and difficult to discern, especially for 1N and 0N, presumably due to their relatively higher crosslink densities resulting from having shorter oligomers on average. 2N appears to exhibit a transition signal at 252 °C, significantly lower than that of PMR-15. 1N may have a T_g at 230 °C and 0N's cannot be identified.

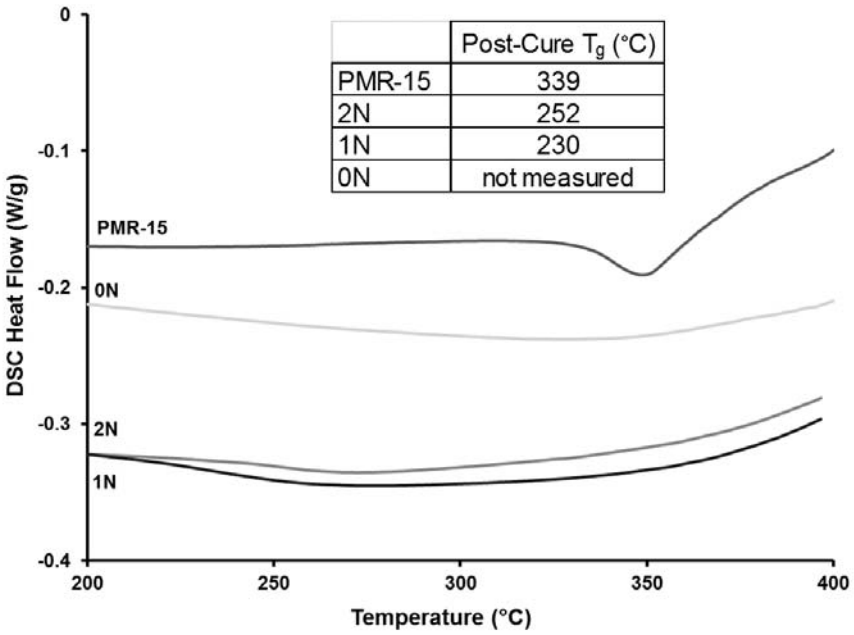

Figure 7. Differential scanning calorimetry (DSC) thermograms of all oligoimides after curing at 315 °C for two hours. Quantified cured glass transitions are tabulated in the inset.

It was discovered in previous studies of 6-FDA-ODA-POSS-PE systems [21] that with higher degrees of POSS in oligomer chains, the more thermal energy was required to render wat could be considered near to full cure. For this work, however, due to the relatively low thermal stability of the PMR-15 framework (BTDA as opposed to 6-FDA, and NA as opposed to PE), increased temperatures for cure was not utilized as a tool to promote further cross-linking. It is therefore plausible to expect that the POSS-containing networks are not what would be considered near or

fully cured. Moreover, IR spectroscopy could not be used as a diagnostic spectroscopic tool to monitor the cure conversion of norbornyl end-caps, as there are no distinct bands corresponding to the reaction products that can be spectroscopically isolated, in contrast with phenyl-ethynyl where the carbon-carbon triple bond has a distinct absorption band, thus facilitating analysis of the kinetics of its consumption.

To gauge the thermal stabilities of this new suite of materials, cured powder (315 °C 90 minutes) was first analyzed by dynamic thermogravimetric analysis (TGA), at a heating rate of 1 °C/minute in inert (gaseous nitrogen) and oxidizing (air) atmospheres, to 600 °C. This slow heating rate was chosen such that an accurate depiction of decomposition events as a function of temperature could be measured. The data in nitrogen is plotted in Figures 8, for normalized residual mass and the derivative of mass loss as a function of temperature. Measurable mass loss begins to occur at ~330 °C, attributed to the disassociation

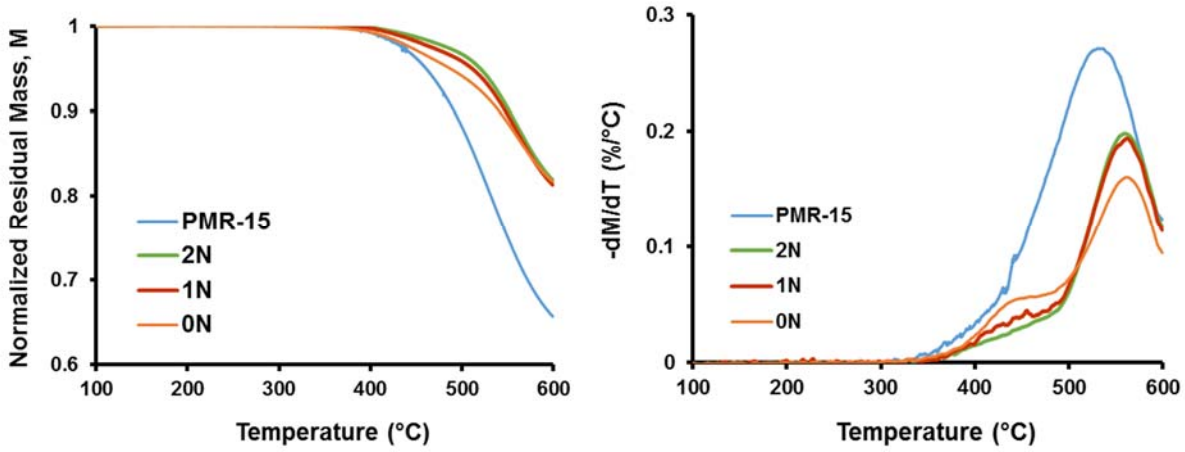

Figure 8. Normalized mass loss profiles (left) and derivative of mass loss (right) as a function of temperature, measured by TGA at 1 °C/minute in a gaseous nitrogen atmosphere. Peaks in the derivative plots designate significant mass loss events.

of the products of the nadic crosslinking group, known to be the weakest species due to its aliphatic character [22-24]. Above 400 °C, in terms of thermal stability characterized by mass

retention, the POSS-containing cured polyimides are more resistant to mass loss than PMR-15. This result suggests that POSS is a more thermally stable segment than MDA in PMR-15. At approximately 475 °C and above, the aromatic rings attached to the POSS cages can participate in co-reactions that produce robust carbonaceous byproducts, likely slowing the mass loss kinetics in that temperature range, also resulting in significantly higher char yields at 600 °C. There is also an obvious trend amongst the POSS-containing networks: thermal stability is inversely proportional to nadic end group concentration (2N>1N>0N). In Figure 8, distinct mass loss events can be distinguished, especially for the POSS-containing networks. For PMR-15, methylene bridge dissociation and associated combination reactions occur in concert with late nadic crosslinking degradation thereby smoothing out the profile.

The general thermal stability trends observed during decomposition in an oxidizing atmosphere are again observed in air in Figure 9. Under thermo-oxidative conditions above 500 °C, the POSS cage can be oxidized to render SiO_2, leaving appreciative residue at 600 °C whereas PMR-15 has been completely decomposed and volatilized. The 0N residue is of highest mass at 600 °C due to its relatively high POSS content in its cured network. Under oxidizing conditions, it has been shown by others that the decomposition of PMR-15 occurs first through the nadic crosslinked groups, followed by the methylene bridge of MDA, and lastly through BTDA [24].

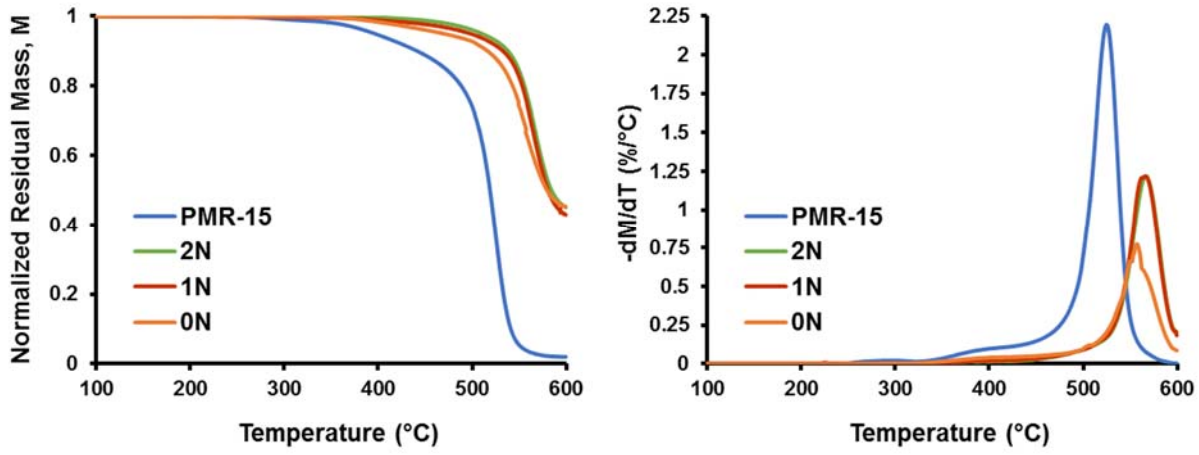

Figure 9. Normalized mass loss profiles (left) and derivative of mass loss (right) as a function of temperature, measured by TGA at 1 °C/minute in air. Peaks in the derivative plots designate significant mass loss events.

To further illustrate the dissimilarities in thermally-induced decomposition attributes and pathways between PMR-15 and the POSS-containing oligomers, the temperatures at which 5 and 10 percent mass losses ($T_{d,5}$ and $T_{d,10}$) occur in the preceding sets of TGA data in both nitrogen and air are plotted in Figure 10 as a function of nadic dianhydride monomer mass fraction. For the POSS-containing materials, these mass loss statistics are a precise linear function of nadic end group concentration, as demonstrate by R^2 values exceeding 0.99. Thus the relative thermal stabilities are 2N>1N>0N. This analysis provides further evidence that the dominant mass loss mechanism in the regime of total mass loss below 10 percent is nadic group decomposition. PMR-15 does not fit this trend. The 5 and 10 percent mass loss temperatures are much lower than expected in the context of nadic end group concentration, suggesting that an additional mass loss mechanism is active. As discovered in the work by Meador et al [24], MDA decomposition occurs early in the degradation process, and the POSS dianiline must therefore be a more stable species.

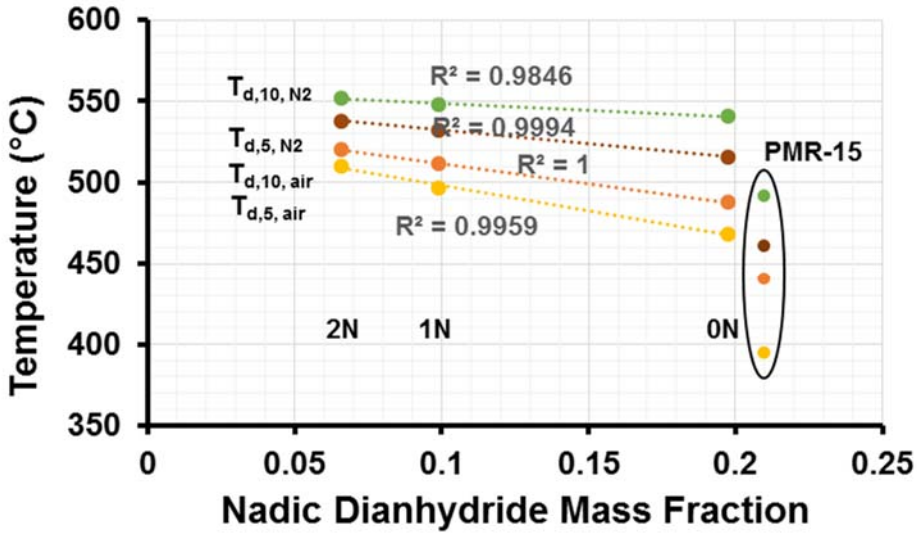

Figure 10. Temperatures at which 5 and 10 percent mass losses (Td,5 and Td,10) occur in both nitrogen and air, plotted against nadic dianhydride mass fraction.

DSC experimentation revealed little to no cure reaction of the nadic end group at 250 °C for sufficiently long periods of time, therefore the rheological characteristics of PMR-15 in comparison with the POSS-containing oligoimides were measured at this temperature via parallel plate oscillatory shear. At a gap spacing of 0.7-0.8 mm, the angular frequency was systematically increased at a strain amplitude of 1%. This complex rheological experiment enables resolution of the storage and loss moduli, which are used to calculate complex viscosity, plotted in Figure 11. PMR-15 exhibits the highest complex viscosity profile at low frequency of 10^9 cP. Replacement of MDA with POSS results in over an order of magnitude lower complex viscosity as evidenced by the profile for the 2N material. For the POSS-containing oligoimides, complex viscosity decreases with molecular weight. The viscosity dependence of the 1N and 2N materials is relatively frequency insensitive in comparison with PMR-15 (having higher interactions between oligomer chains) and 0N (very low level of interactions). It is evident that POSS reduces inter-oligomeric contact, acting to increase free volume in the liquid (and likely solid) states. These results suggest that processability reflected by flow viscosity as a function of temperature is reduced and thereby positively influenced by POSS. Further analysis is provided in Supporting Information.

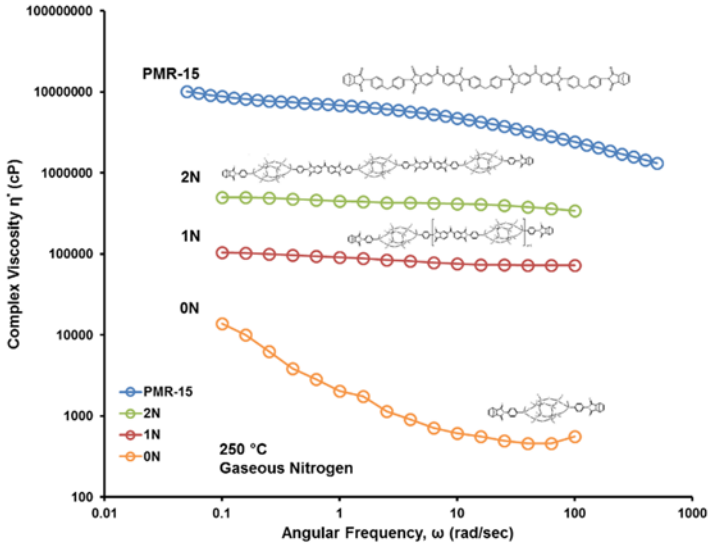

Figure 11. Complex viscosity as a function of angular frequency at 250 °C, a gap spacing of 0.7-0.8 mm, and oscillatory strain of 1%.

Using staging techniques, disks were successfully fabricated from all of the oligomers. Characterization activities on these specimens were performed on one disk of each composition including density, viscoelastic characterization by TMA (non-destructive), moisture uptake and diffusion (non-destructive), followed lastly by thermo-oxidative (TOS) stability (destructive).

The average densities of the cured oligoimide networks, resulting from three measurements, are tabulated below. PMR-15 exhibits the highest density while the POSS-containing materials have values that correlate with POSS mass fraction. With increasing POSS content, density decreases, in spite of assumed increased crosslink density resulting from the shortened chain lengths in 1N and 0N, in comparison with 2N. This finding expectedly suggests that POSS dominates network architecture due to the large volume that it occupies in relation to BTDA and NA.

Table 4. Average densities resulting from three measurements on each cured disk. Values were measured by immersion in methanol on a balance.

Material	Average Density (g/cm^3)	Standard Deviation
PMR-15	1.284	0.0121
2N	1.268	0.0184
1N	1.253	0.0140
0N	1.238	0.0028

The results from dynamci TMA scans are plotted in Figure 12 a-d, respectively, after pre-heating the disks in-situ to 350 °C to baseline their thermal histories and to promote residual

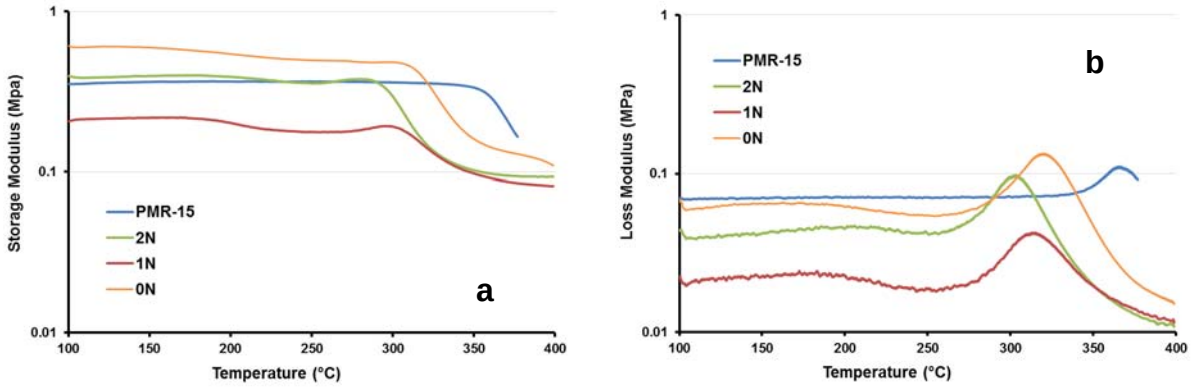

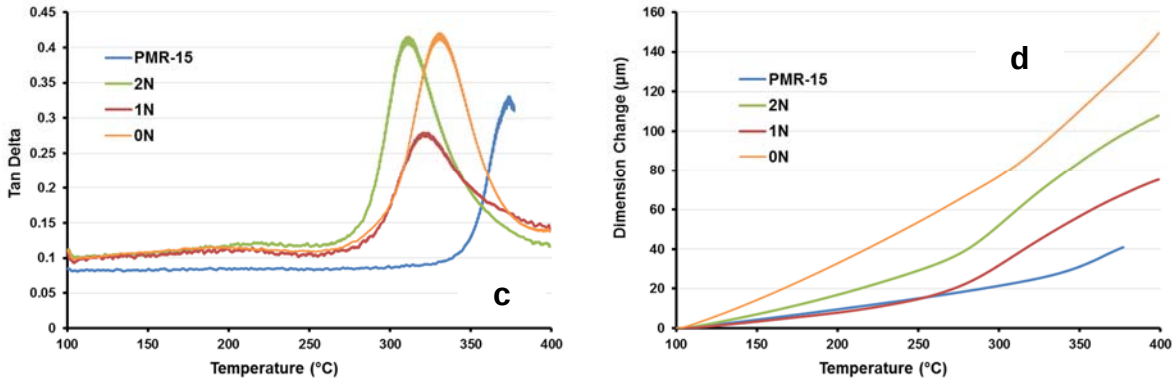

Figure 12. Plots of storage modulus, G′ (a), loss modulus, G″ (b), tan delta, δ (c), and coefficent of thermal expansion, CTE, (d).

cure, followed by cooling to 50 °C in preparation for the final sweep. To preface data analysis, 2N, 1N, and 0N all feature the same weight fraction of POSS (0.80), but differ in average chain length and POSS volume conentration, affecting the distance between cross-link junctions in the cured state. First, it is apparent that all datasets converge to PMR-15 demonstrating the highest T_g (quantified in Table 5) no matter what form of measurement. Co-oligomerization with POSS clearly lowers T_g, successfully offest to some degree by shortening oligomer chain length. Also common amongst the POSS family of oligomers is a weak relaxation event activated just above 200 °C, possibly attributed to POSS cage excitation. POSS also generally increases CTE, especially after the transition from a glassy to rubbery state. All of the cured networks demonstrate tan δ below 0.2 except in the transition region, indicative of highly crosslinked thermoset networks. The 1N cured network exhibits somwehat anomolous behavior with a less steep transition into the rubbery plateau and lower CTE in the pre-transition state, as well as lower tan δ in the transition region. These results suggest a possibly higher degree of cure, perhaps due to a balance in thermal induced molecular mobility and optimized oligomer segment length, but steadfast conclusions

cannot be drawn from one set of experiments. This behavior could be due to experimental error of specimen imperfections in the contact surface, etc.

Table 5. Quantified values of the glass transition temperature (Tg) as measured from the salient characteristics of storage modulus (G′), loss modulus (G″), tan delta (δ), and coefficent of thermal expansion (CTE).

	Tg (°C)			
	Storage Modulus	**Loss Modulus**	**Tan Delta**	**Dimension Change**
PMR-15	343	366	374	319
2N	288	303	312	274
1N	301	315	321	265
0N	304	315	326	293

Water uptake data is plotted in Figure 13. The behavior of the POSS-containing materials is remarkably different than that of PMR-15. Diffusion is a much more gradual process for PMR-15, reaching saturation at approximately 24 hours, with a mass gain of 4.3%. The POSS materials reach saturation within a single hour, but the mass gain is 4 times less, with 2N gaining 0.93%, 1N 1.1%, and 0N 1.25%, highlighted for comparison in Figure 14. Saturated mass gain correlates to density mongst the POSS materials in that 0N takes up the most water, albeit a marginal difference. Although it may be concluded that more porous

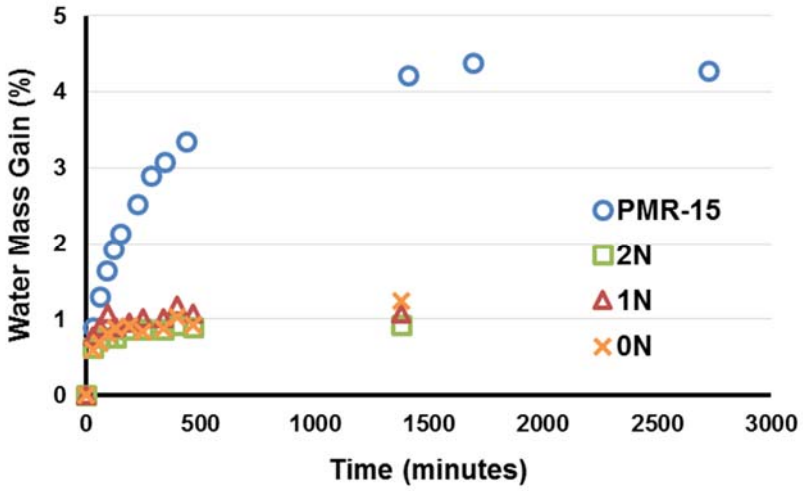

Figure 13. Moisture diffusion profiles for the cured polyimide networks during boiling water immersion.

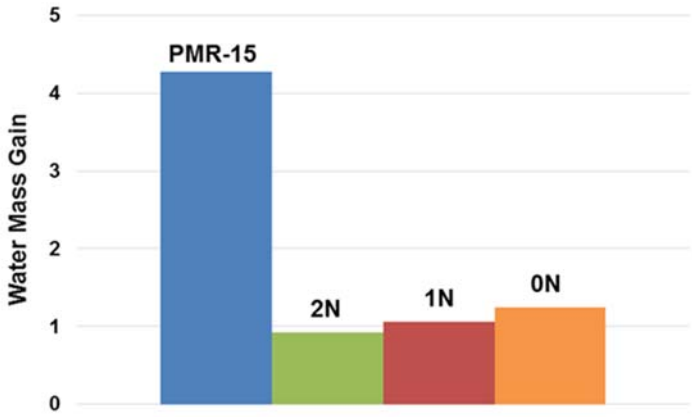

Figure 14. Bargraph chart comparing the saturated moisture uptake in the cured polyimide networks after boiling water immersion.

networks such as that of 0N can accommodate more water molecules for the POSS polyimides, this does not hold true when examining PMR-15, which exhibits the lowest density of all but by far the highest mass gain. The imide and carbonyl groups of PMR-15 are polar and are known to participate in inter-chain interactions with each other (termed charge transfer complexing, or CTC interactions). These sites have been shown to have a propensity for hydrogen bonding with water

molecules [25]. During the process of water infiltration and hydrogen bonding, polyimides have been shown to expand through long range translational chain motion processes that allow for more water to be accomodated, forming dimers or greater degrees of coalescence. Although this phenomena is likely to explain the behavior of PMR-15, it does not appear to hold for the POSS-containing networks due to the rapidity of water ingress to saturation. The data suggests that water molecules enter the POSS-containing networks very quickly to occupy avialable volume, rather than long diffusion-dominated processes. This hypothesis is supported by the observance of marginal diffrences in saturated uptake based on cured network density. It is further postulated that water molecules cannot generally hydrogen bond with carbonyl and imide groups in the POSS-containing materials as they may be shielded by the relatively large cage structure and peripheral phenyl groups. Although the POSS-containing networks are less dense than PMR-15, the free volume introduced by POSS may not be largely accessible to water molecules, and this may be largely due to the aromatic peripheral groups. It would be informative to understand the state of the networks and how they are affected by POSS, which could be the subject of thermoset cure modeling, but was beyond the scope of this effort.

A benefit from increased moisture diffusion coefficients is that diffused water molecules in composite structures can more easily escape during rapid heating with less probability of damaging the structure. In essence, POSS appears to render more breathable resin network structures, but does not result in increased saturated moisture content, but rather a resistance to significantly higher water occupation as seen with PMR-15. Unfortunately, if water molecules can more readily penetrate a network, so can oxygen during exposure of composites to elevated service temperatures. To quantify long-term thermos-oxidative stability (TOS), the cured disks were dried after the boiling water immersion studies back to their equilibrium masses. The disks were situated

on an aluminum mesh positioned on a graphite boat and inserted into a tube furnace with flowing air of purity and controlled rate. The temperature was set at 316 °C to accelerate aging processes. The specimens were periodically removed from the furnace and weighed to determine their weight loss. The results are plotted in Figure 15. For each data set, three regimes of mass loss can be distinguished: 1) initial non-linear accelerated loss, 2) linear gradual loss, and 3) slowed loss at long exposure times. The slopes of the linear portions of the mass loss data sets are readily quantified to be PMR-15 (3×10^{-3} %/hr), 2N (2.2×10^{-3} %/hr), 1N (2.6×10^{-3} %/hr), and 0N (7.8×10^{-3} %/hr). The mass loss rate of 2N and 1N are lower than PMR-15 in the linear regime, while that of 0N is higher. These rates likely stem from nadic crosslink concentration in the networks, as described in the TGA data analysis section, as 2N>1N>0N in terms of relative stability.

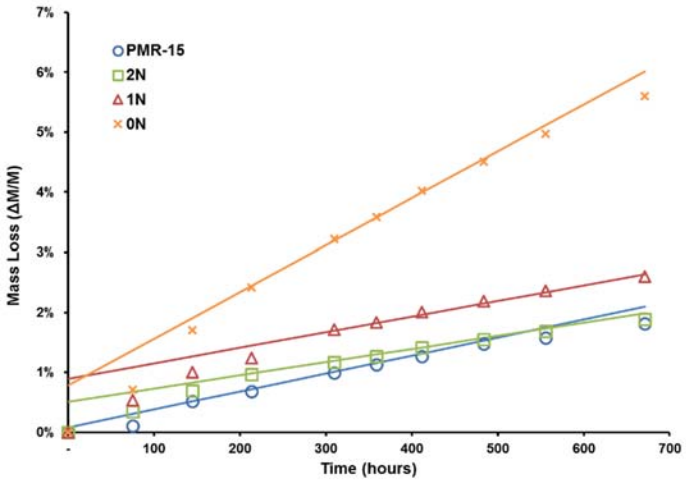

Figure 15. Mass loss profiles for the cured polyimide networks as a function of exposure time to 316 °C and flowing air conditions precisely controlled in a tube furnace.

Two key features of the 0N resin system mechanical property data were of interest for further study: adhesion of this resin to carbon fiber as the primary constituent is POSS which might be expected to have a greater affinity for glass over carbon, and reduced toughness of the resin system due its relatively high crosslink density, which was implemented in an attempt to offset

reduced T_g. Therefore, ASTMs D 2344 (short beam or interlaminar shear) and D 7264 (flexural strength) were chosen as test methods. Three samples of PMR-15 and 0N composite were tested to failure by ASTM D 7264, the results of which are shown in Table 6. The average flexural strength for PMR-15/IM7-8HSW-GP is ~1850 MPa, much higher than the literature value of 1082 MPa with T650-35, because the latter is a unidirectional textile tape rather than a woven fabric, the former providing greater flexural resistance. The average flexural strength of the 0N/IM7-8HSW-GP composite is 405 MPa, 78% less than that of its PMR-15 counterpart. The most significant contribution to this drastic reduction in flexural strength is crosslink density of the resin matrix. The 0N resin's crosslink density is much higher than that of PMR-15, inducing embrittlement. The interlaminar shear strength (ILSS) determined from short beam shear testing is also presented in Table 6. The average ILSS strength of PMR-15/IM7-8HSW-GP is 77 MPa, while that of 0N/IM7-8HSW-GP is 22 MPa, 71% less. This knockdown is likely attributed to poor adhesion of the 0N resin system to either the GP (epoxy-based) sizing or the carbon fiber itself. This result is worth continued exploration, because POSS has been used by others as an interfacial strength promoting agent between high temperature resin systems and carbon fiber [26].

Table 6. Results from flexural and short beam shear testing of PMR-15 and 0N composites containing Hexcel 8 harness satin weave IM7 carbon fiber fabric.

		PMR-15	**0N**
Flexural Strength	ksi (st. dev.)	268.1 (66.2)	58.8 (111.1)
	mpa (st. dev.)	1848.7 (456.3)	405.4 (76.4)

Flexural Modulus	ksi (st. dev.)	111.6 (46.1)	72.2 (20.2)
	mpa (st. dev.)	769.8 (318.1)	497.8 (139.3)
Interlaminar Shear Strength	ksi (st. dev.)	11.1 (0.2)	3.2 (0.3)
	mpa (st. dev.)	76.8 (1.1)	22.3 (1.9)

The long-term TOS of composites prepared from PMR-15, 0N, and IM7-8HSW-GP was examined at 316 °C, in the same manner as that used for neat resin specimens, and is plotted in Figure 16. Mass loss data was collected to 625 hours. Similar to the resin specimens, the composites demonstrate a period of acceleration of weight loss up to 100 hours, after which a long period of steady linear loss transpires out to ~500 hours, lastly followed by a period of slower loss. In the linear regime, the mass loss rates are readily calculated for comparison. The rate of loss for PMR-15/IM7-8HSW-GP is 1.1×10^{-5} (%/hr), while that of 0N/IM7-8HSW-GP is 4.0×10^{-5}. The rate of mass loss contrast between the composites is 4, while that of the neat resin specimens of PMR-15 and 0N is 3, therefore in compositized form the mass loss in 0N/IM7-8HSW-GP could be exacerbated by increased void content, or poor adhesion between fiber and matrix leaving a path of free volume for oxygen to attack the composite.

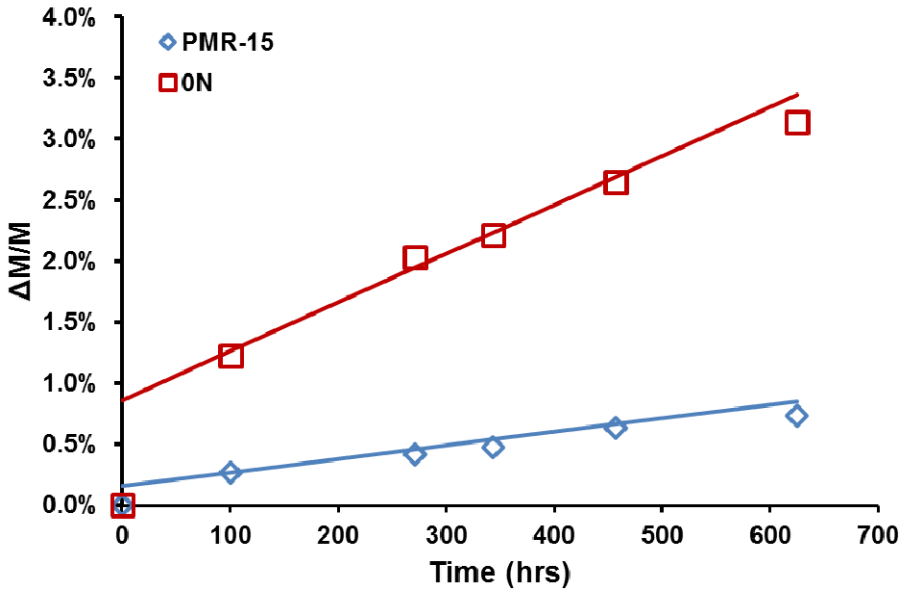

Figure 16. Long-term thermo-oxidative stability mass loss measurements at 316 °C for the PMR-15 and 0N/IM7-8HSW-GP composites.

The cross sections of the composite specimens were imaged using a digital microscope before, during, and after TOS exposure. The pre-test micrographs for PMR-15 and 0N/IM7-8HSW-GP are shown in Figure 17. Few flaws are seen in the PMR-15 composite, while some voids near the surface of the 0N composite are present. Images after 625 hours at 316 °C are presented in Figure 18. For PMR-15, several large in-plane and transverse cracks have manifested, which are known to seriously degrade mechanical properties. Remarkably, the 0N composite exhibits no microcracking or other flaws which may be attributed to TOS aging, despite its relatively higher mass loss. It is suspected that the POSS cage, due to its slight flexibility, may act to dampen strains in the network caused by thermal, aging, and degradation-induced stresses, although other potential causes, such as differences in the extent of cure for the specimens, must also be taken into account in order to make a more definitive comparison.

Figure 17. Pre-TOS test optical micrographs for PMR-15/IM7-8HSW-GP (upper) and 0N/ IM7-8HSW-GP (lower) composite cross-sections.

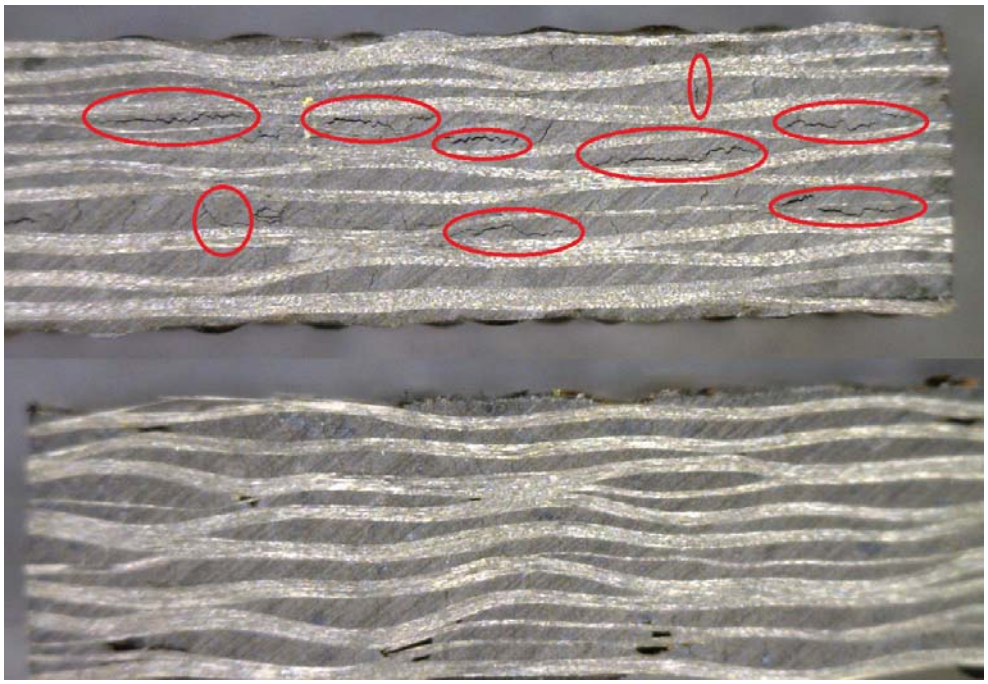

Figure 18. Post-TOS optical micrographs for PMR-15/IM7-8HSW-GP (upper) and 0N/ IM7-8HSW-GP (lower) composite cross-sections after 625 hours at 316 °C. The PMR-15 composite has grown microcracks while that from 0N has not.

Conclusions

The viability of co-oligomerization of a POSS dianiline monomer designed to be highly thermally stable was studied. Co-oligomerization was found to significantly improve processability marked by viscosity decrease. Composite laminates were fabricated with a POSS-containing oligomer without the use of solvent or need for prepregging. Microscopic observation of thermally degraded samples revealed a lack of expected micro-cracking in the resin after high-temperature oxidation, an interesting result that merits more detailed study. However, due to a large volumetric molecular footprint, incorporation of POSS increases network free volume to the extent that the cured network glass transition temperature is significantly reduced. In attempts to mitigate this effect, crosslink density was increased to the extent that the resin suffered embrittlement, and the nadic crosslink concentration diminished thermal stability as this is the weak link in the network. Although all results indicate that network free volume is increased when POSS is incorporated into the architecture, a substantial decrease in moisture uptake was observed in comparison with other commercial polyimide systems, reducing the risk of composite structure failure due to rapid moisture release and knockdowns in mechanical and viscoelastic properties.

References

1. T.T. Serafini, P. Delvigs, G.R. Lightseg, J Appl Polym Sci, 1972, 16, 905.
2. P.J. Cavano, W.E. Winters, "PMR Polyimide/Graphite Fiber Composite Fan Blades," NASA CR-135113, pp. 5-6, December 1976.
3. P. Delvigs, W.B. Alston, R.D. Vannucci, "Effects of Graphite Fiber Stability on the Properties of PMR Polyimide Composites," NASA TM-79062, AVRADCOM TR 78-62, May 1979.
4. W.B. Alston, "Resin/Fiber Thermo-Oxidative Interactions in PMR Polyimide/Graphite Composites," NASA TM-79093, AVRADCOM TR 79-6, May 1979.

5. F. P. Guengerich, J Biochem Mol Toxic, 2007, 21, 163-168.

6. F. P. Guengerich, Chem Res Toxicol, 2008, 21, 70-83.

7. C. H. Yun, T. Shimada and F. P. Guengerich, Carcinogenesis, 1992, 13, 217-222.

8. A. G. Siraki, T. S. Chan, G. Galati, S. Teng and P. J. O'Brien, Drug Metab Rev, 2002, 34, 549-564.

9. R. W. Scholz, K. S. Graham, E. Gumpricht and C. C. Reddy, Ann Ny Acad Sci, 1989, 570, 514-517.

10. R. E. Hughes, Nature, 1964, 203, 1068.

11. H. Kopelman, M. H. Robertson, P. G. Sanders and I. Ash, Br Med J, 1966, 1, 514-516.

12. Chuang, K. "High Tg Polyimides", NASA Tech Report 563972, 2002.

13. Vij, V.; Haddad, T. S.; Yandek, G. R.; Ramirez, S. M.; Mabry, J. M. "Synthesis of Polyhedral Oligomeric Silsesquioxane (POSS) Dianilines for use in High-Temperature Polyimides", Silicon, 2012, 4, 267.

14. McCusker, C.; Carroll, J. B.; Rotello, V. M. Chem. Comm. 2005, 996-998.

15. Skaria, S.; Schriker, S. ACS Polymer Preprints 2005, 46(1), 94.

16. Kannan, R. Y.; Salacinski, H. J.; Butler, P. E.; Seifalian, A. M. Acc. Chem. Res. 2005, 38, 879-884.

17. Kannan, R. Y.; Salacinski, H. J.; De Groot, J.; Clatworthy, I.; Bozec, L.; Horton, M.; Butler, P. E.; Seifalian, A. M. Biomacromolecules 2006, 7, 215-223.

18. Kannan, R. Y.; Salacinski, H. J.; Odlyha, M.; Butler, P. E.; Seifalian, A. M. Biomaterials 2006, 27, 1971-1979.

19. Punshon, G.; Vara, D. S.; Sales, K. M.; Kidane, A. G.; Salacinski, H. J.; Seifalian, A. M. Biomaterials 2005, 26, 6271-6279.

20. http://www.dailymail.co.uk/sciencetech/article-2266689/Cancer-victim-growing-new-nose-arm-Businessman-lost-organ-disease-hopes-new-sewn-face.html

21. Pinson, D. M.; Yandek, G. R.; Haddad, T. S.; Horstman, E. M.; Mabry, J. M. Macromolecules 2013. 46 (18), pp 7363-7377.

22. Malarik, D. C.; Vannucci, R. D. NASA Technical Memorandum 105364, December, 1991.

23. Sutter, J. K.; Jobe, J. M.; Crane, E. A. J. Appl. Polym. Sci. 1995, 57, 1491-1499.

24. Meador, M. A. B.; Johnston, J. C. Macromolecules 1997, 30, 3215-3223.

25. Mensitieri, G.; Lavorgna, M.; Larobina, D.; Scherillo, G.; Ragosta, G.; Musto, P. Macromolecules 2008, 41, 4850-55.

26. By Zhang, Xuezhong; Huang, Yudong; Wang, Tianyu; Hu, Lijiang. Journal of Materials Science 2007, 42(13), 5264-5271.